C-terminal mutants of *C. elegans* Smads reveal tissue-specific requirements for protein activation by TGF-β signaling

Jianjun Wang[1,2], William A. Mohler[2] and Cathy Savage-Dunn[1,*]

[1]Department of Biology, Queens College, and the Graduate School and University Center, the City University of New York, 65-30 Kissena Boulevard, Flushing, NY 11367, USA
[2]Department of Genetics and Developmental Biology, University of Connecticut Health Center, 263 Farmington Avenue, Farmington, CT 06030, USA
*Author for correspondence (e-mail: csavage@qc1.qc.edu)

Accepted 6 June 2005

Development 132, 3505-3513
Published by The Company of Biologists 2005
doi:10.1242/dev.01930

Summary

TGF-β signaling in the nematode *Caenorhabditis elegans* plays multiple roles in the development of the animal. The Sma/Mab pathway controls body size, male tail sensory ray identity and spicule formation. Three Smad genes, *sma-2*, *sma-3* and *sma-4,* are all required for signal transduction, suggesting that the functional complex could be a heterotrimer. Because the C termini of Smads play important roles in receptor-mediated activation and heteromeric complex formation, we generated C-terminal mutations in the *C. elegans* Smad genes and tested their activities in vivo in each of their distinct developmental roles. We show that pseudophosphorylated SMA-3 is dominant negative in body size, but functional in sensory ray and spicule development. Somewhat differently, pseudophosphorylated SMA-2 is active in any tissue. The C-terminal mutants of SMA-4 function like wild type, suggesting that the SMA-4 C terminus is dispensable. Using a combination of different C-terminal mutations in SMA-2 and SMA-3, we found a complex set of requirements for Smad-phosphorylation state that are specific to each outcome. Finally, we detected a physical interaction of SMA-3 with the forkhead transcription factor LIN-31, which is enhanced by SMA-3 pseudophosphorylation and reduced in an unphosphorylatable mutant. We conclude that the tissue-specific requirements for Smad phosphorylation may result, in part, from the need to interact with tissue-specific transcription co-factors that have different affinities for phosphorylated and unphosphorylated Smad protein.

Key words: Body size, Pattern formation, Phosphorylation, Smad, TGF-β, *C. elegans*

Introduction

TGF-β-related ligands, including the BMP subfamily, control the development of metazoans by regulating cellular processes that include cell growth, cell differentiation, apoptosis and proliferation. In humans, components of the TGF-β pathway play important roles as tumor suppressors (Wakefield and Roberts, 2002). From the cell membrane to the nucleus, the signal is transduced by type I and type II transmembrane SER/THR kinase receptors and intracellular Smads, which are conserved among both invertebrates and vertebrates (Savage-Dunn, 2001; Shi and Massagué, 2003). The receptor-regulated Smad proteins (R-Smads) are phosphorylated by the activated type I receptor and form a complex with co-mediator Smad (Co-Smad, namely Smad4). The complex enters the nucleus to regulate the transcription of target genes (Attisano and Wrana, 2002; Moustakas et al., 2001; Massagué and Wotton, 2000). Smad proteins contain two highly conserved regions, the MH1 and MH2 domains, located at the N and C termini, respectively, connected by a linker region. The linker region is not highly conserved and could be the target of activity modulation (Hata et al., 1997; Massagué, 2003).

Two serines/threonines at the C terminus of R-Smad proteins (consensus sequence SS*XS*) are the substrates of receptor phosphorylation (Abdollah et al., 1997; Souchelnytskyi et al., 1997). Phosphorylation is thought to relieve autoinhibition of the MH2 domain by the MH1 domain, allowing Smad complexes to form and translocate to the nucleus (Hata et al., 1997). The crystal structures of homomeric complexes containing Smad1 or phosphorylated Smad2 (pSmad2), and of heteromeric complexes containing pSmad2:Smad4 or pSmad3:Smad4, have provided insight into the structural basis of complex formation (Qin et al., 2001; Wu et al., 2001b; Chacko et al., 2004). The crystal structures show that the phosphorylated C terminus of each R-Smad subunit binds a positively charged pocket of another subunit (Wu et al., 2001b; Chacko et al., 2004). Other studies have shown that pseudophosphorylation of R-Smads by the substitution of negatively charged amino acids for C-terminal serines can result in their activation independently of exogenous ligand (Liu et al., 1997; Petritsch et al., 2000; Chacko et al., 2001; Qin et al., 2001). Somewhat paradoxically, in other contexts, pseudophosphorylated R-Smads (ppR-Smads) were found to have dominant-negative effects (Liu et al., 1997; Souchelnytskyi et al., 1997; Petrisch et al., 2000). Nevertheless, the functional consequences of Smad phosphorylation have not been extensively addressed in any intact organism.

The core TGF-β signaling components have been identified in *Caenorhabditis elegans*, providing a genetically tractable model system for their study. There are multiple TGF-β-related pathways that control different events in *C. elegans* development. The Sma/Mab and Dauer pathways regulate body size and dauer formation, respectively (Patterson and Padgett, 2000; Savage-Dunn, 2001). These two pathways share one type II receptor, DAF-4, but the type I receptors, SMA-6 and DAF-1, are pathway specific. When *daf-4* is transformed into human cell lines, the *C. elegans* receptor protein binds vertebrate BMP ligands showing conservation between these pathway components in human and *C. elegans* (Estevez et al., 1993). Loss of function of the Sma/Mab pathway results in a small body size. Furthermore, in the male tail, some of the sensory rays become fused and the spicules are crumpled (Savage et al., 1996). A model for Sma/Mab pathway signaling has been developed on the basis of analogy with biochemical experiments in other systems. The ligand DBL-1 interacts with the type II receptor DAF-4 and the type I receptor SMA-6. The intracellular Smad homologs SMA-2, SMA-3 (R-Smads), and SMA-4 (Co-Smad), propagate the signal, presumably by forming complexes that accumulate in the nucleus. In the nucleus, the Smads may interact with tissue-specific transcription co-factors, such as LIN-31 (Baird and Ellazar, 1999) and SMA-9 (Liang et al., 2003). We have previously shown that *sma-3* is expressed in the pharynx, intestine and hypodermis. Expression in the hypodermis is necessary and sufficient to regulate body size. Also, pathway activity activates a negative-feedback loop that reduces SMA-3 protein accumulation (Wang et al., 2002).

We have noted that SMA-3 does not function well with GFP attached to the C terminus, suggesting that the C terminus of SMA-3 is crucial for its activity (Wang et al., 2002). As the C terminus is likely to be the site of phosphorylation, we reasoned that mutating C-terminal residues could provide an opportunity to investigate the roles of Smad phosphorylation in vivo. We have therefore generated C-terminally mutated *sma-3* genes by site-directed mutagenesis. Our results indicate that Smad phosphorylation at the C terminus is not required for nuclear accumulation, but is probably required for Smad complex formation and for interaction with transcription co-factors. We also find that different developmental processes show a differential tolerance for Smad C-terminal modification. These differences may be due in part to the need for interaction with tissue-specific transcription co-factors that have different affinities for unphosphorylated or pseudophosphorylated Smads. Finally, we have created wild-type rescuing and pseudophosphorylated *sma-2* constructs that function differently from the *sma-3* variants. These data, from both *sma-2* and *sma-3*, reveal some of the complex and sophisticated signaling mechanisms by which the Sma/Mab pathway produces tissue-specific developmental outcomes.

Materials and methods

General methods and worm strains

C. elegans strains were cultured as described by Brenner (Brenner, 1974). The following strains were used: wild-type *C. elegans* variety Bristol strain N2; LGII *sma-6(wk7)*; LGIII, *sma-2(e297)*, *sma-3(wk30)*, *sma-4(e729)*, *lon-1(wk50)*, *sma-3(e491)sma-2(502)*; LG V, *him-5(e1490)*.

Cloning of genomic *sma-2*

The *sma-2* ORF is contained within a large genomic region. One large intron (3 kb) contains another gene. It is unknown whether this gene has any relationship with *sma-2*. A second large intron (intron 7, 1 kb) near the 3′ end contains an interesting sequence. The first half is complementary to the second half. During PCR, this intron creates aberrant products. The final rescuing genomic clone, pCS309, does not include these two introns. This clone was assembled from four PCR products using the following primers (underlined bases indicate engineered restriction sites):

upstream sequences, AAGGTACCGGCAGTAGCTTCTCCTTGTC and AAGTCGACTAATAGTCACAAGAAGATTC;

5′ end, AACTGCAGATTAGAATCATGGTAAGT and AAGATATCGTAAAATTAACGTTTGCCAT;

3′ end (before intron 7), AACCCGGGAGCCAACCAATTTCATCAAT and AACCATGGACTCAAACATTGCAATTACG; and

3′ end (after intron 7), AACCATGGACCCGGAACTTATTTGGAG and ATGGCGCCGCTCAAGAAATTGAAGAAATTGGCC.

This strategy resulted in the insertion of six nucleotides encoding two amino acids between the 5′ and 3′ ends of the gene, due to the engineered restriction sites in the primers. The full predicted sequence of pCS309 is available upon request.

Site-directed mutagenesis

Using the MutaGene kit from BioRad, *sma-3* C-terminal mutations were generated by adding primers complementary to the uracil-containing single-strand DNA purified from the CJ236 *E. coli* strain. After extending by T7 DNA polymerase and ligating by T4 ligase, the DNA was transformed and amplified in the DH5α *E. coli* strain. The mutations were confirmed by DNA sequencing.

Primers for *sma-3* mutagenesis:

DME, GGAACCAATGACATGGAATAATGATT;

AMA, GGAACCAAATGCAATGGCATAATGATT; and

Deletion, CGAACTTCATYGAACCAAATTAATGATTTGTTAAAA.

By chance, we also generated a deletion of MT. The C-terminal mutations of *sma-2* and *sma-4* were generated by PCR using primers containing the mutations. The 5′ primers were normal and the 3′ primer sequences were:

*sma-2*DID, 3′ ATGCGGCCGCTAATCAATATCAGAAATTGGCCGTGGAGT;

*sma-4*AA, 3′ AATCTAGATTATGCTGCTCCAAATTGAGAACTATTTT;

*sma-4*DD, 3′ AATCTAGATTAGTCATCTCCAAATTGAGAACTATTTT;

*sma-4*SSIS, 3′ AATCTAGATTATGATATGGAACTTCCAAATTGAGAAC.

Transformation and integration

All of the DNA constructs were amplified in the DH5α *E. coli* strain and purified by mini-prep kit (Qiagen). The DNA concentration for injection is 20 μg/ml using 100 μg/ml *rol-6* marker gene (Mello et al., 1991). For each transformation, at least three lines were observed and data are shown for one representative line. Integration of extrachromosomal arrays was carried out by exposure to 4000 Rad of gamma ray from a ^{137}Cs source, as described previously (Wang et al., 2002).

Body-length measurement and male tail analysis

Eggs were collected from gravid hermaphrodites by bleaching with hypochlorite solution for 5 minutes. After the eggs were centrifuged and cleaned by M9 buffer, they were spread onto new plates. At 96 hours after egg collection, the photos were taken and body lengths were measured using SigmaScan software. The males from non-starved plates were picked at young adult stage. The male tail sensory rays were visualized by Nomarski DIC optics using a Zeiss Axioplan and the defects were scored.

Yeast two-hybrid assay

The cDNAs of interaction partners were cloned into pPC86 and pPDLeu yeast vectors. Competent cells of the yeast strain Mav203 were cultured at 30°C until the OD value was about 0.5. After centrifugation, ice-cold 0.1 M LiCl was added. The transformation was conducted by adding 5 μg boiled salmon sperm DNA, 0.1 M lithium acetate, 10% PEG 3350. After adding the DNA and heat shocking at 42°C for 5 minutes, the yeasts were incubated at 30°C for 30 minutes and spread onto plates without Trp or Leu. The interaction was determined by spreading the transformed yeast onto the plates with 25 mM or 50 mM 3AT without His.

Results

sma-3 C-terminal mutants fail to rescue small body size

SMA-2 and SMA-3 have sequence homology with mammalian R-Smads. The C-terminal sequence of SMA-3 NSMT is a variant of the canonical SSXS motif. As the last two serines of R-Smads are phosphorylated during activation (Abdollah et al., 1997; Souchelnytskyi et al., 1997), SMA-3 is likely to be phosphorylated on the terminal serine and threonine residues. To test the role of phosphorylation of the SMA-3 C terminus, we generated *sma-3* mutant variants (Table 1). We hypothesized that the pseudophosphorylated DME mutation (ppSMA-3) might be activated without upstream signaling. Conversely, the unphosphorylatable AMA mutation was expected to be nonfunctional in all tissues. Finally, we also generated *sma-3* deletion mutants by removing SMT or MT. To test the activities of these mutant Smads, we introduced the constructs into *sma-3(wk30)* mutants, which carry a null allele containing a premature termination codon in *sma-3* (Savage-Dunn et al., 2000). To test for rescue of the small body size, body length was measured in adulthood, 96 hours after egg collection at 20°C. Surprisingly, none of these constructs is functional in rescuing the body size (Table 2). Most strikingly, ppSMA-3 failed to rescue. This result suggests that true phosphorylation of SMA-3 (pSMA-3) is required for body size control. The non-functional C-terminal deletions suggest both C-terminal serine and threonine residues are required for SMA-3 activity.

SMA-3 C-terminal mutant forms are expressed normally

We previously reported that *sma-3* is expressed in hypodermis, pharynx and intestine from late embryo through the larval and adult stages. When a GFP tag is attached to the N terminus of SMA-3, the fusion protein is still functional and accumulates in the nucleus (Wang et al., 2002). We tagged our SMA-3 mutant forms with N-terminal GFP. All of these mutated proteins were expressed normally and were nuclear localized (Fig. 1 and data not shown). Although the AMA site could not be phosphorylated by SMA-6, the presence of SMA-3 AMA in the nucleus is consistent with our previous finding that phosphorylation is not necessary for nuclear localization. The other dominant-negative constructs have similar localization, but the fluorescence intensity is much lower.

Table 1. The designed C-terminal mutants of SMA-2, SMA-3 and SMA-4

Proteins	C terminus	Description
SMA-3	SMT	Wild type
	DME	Pseudophosphorylated
	AMA	Non-phosphorylatable
	ΔMT	Partially functional
	ΔSMT	Non-functional
SMA-2	SIS	Wild type
	DID	Pseudophosphorylated
SMA-4	SS	Wild type
	DD	Pseudophosphorylated
	AA	Non-phosphorylatable
	SSIS	Simulate R-Smad

sma-3 C-terminal mutants are dominant negative in body size regulation

Interestingly, the integrated arrays with the mutated *sma-3* genes were dominant negative in body size regulation when crossed into a wild-type background (Table 2). This suggests that these constructs interfere with the function of the wild-type *sma-3* gene. During the cross, we observed that the heterozygotes of the integrated array are a little longer than homozygotes (data not shown), suggesting that the inhibition is dose dependent. The SMA-3 DME mutant, which we expected to be constitutively active, is instead a strong inhibitor of growth. The SMA-3 AMA is the weakest one among the dominant negatives. We can postulate at least two different mechanisms for the inhibition. First, the mutated SMA-3 proteins could compete with wild-type SMA-3 by binding to the receptors or other Smad proteins. Alternatively, although these SMA-3 mutants are not functional in body size

Table 2. The effects of *sma-3*, *sma-2* and *sma-4* mutations on body size

Strain	Transgenes*	Body size (mm)†	*n* (worms)
sma-3(wk30)	None	0.73±0.04	80
	qcIs19(sma-3 wt)	1.19±0.10	90
	qcIs7(sma-3 DME)	0.75±0.06	42
	qIs15(sma-3 AMA)	0.66±0.04	60
	qcIs5(sma-3 ΔMT)	0.74±0.05	54
	qcIs4(sma-3 ΔSMT)	0.73±0.05	42
N2	None	1.17±0.08	30
	qcIs7(sma-3 DME)	0.72±0.06	39
	qIs15(sma-3 AMA)	0.84±0.05	56
	qcIs5(sma-3 ΔMT)	0.74±0.04	45
	qcIs4(sma-3 ΔSMT)	0.79±0.06	44
lon-1(wk50)	None	1.36±0.11	30
	qcIs15(sma-3 DME)	0.93±0.05	31
	qcIs15(sma-3 AMA)	1.10±0.07	36
	qcIs5(sma-3 ΔMT)	1.00±0.05	44
	qcIs4(sma-3 ΔSMT)	1.06±0.06	34
lon-1(wk50) sma-3(wk30)	None	1.24±0.07	52
sma-2(e297)	None	0.77±0.06	33
	qcIs39(sma-2 wt)	1.19±0.09	45
	qcIs41(sma-2 DID)	1.07±0.09	30
sma-4(e729)	None	0.79±0.05	40
	qcEx58(sma-4 wt)	1.19±0.07	42
	qcEx59(sma-4 AA)	1.18±0.07	38
	qcEx60(sma-4 DD)	1.19±0.08	32
	qcEx61(sma-4 SSIS)	1.21±0.09	34

*All transgenes include the *rol-6* marker.
†Body size: average length±s.d. at 96 hours.

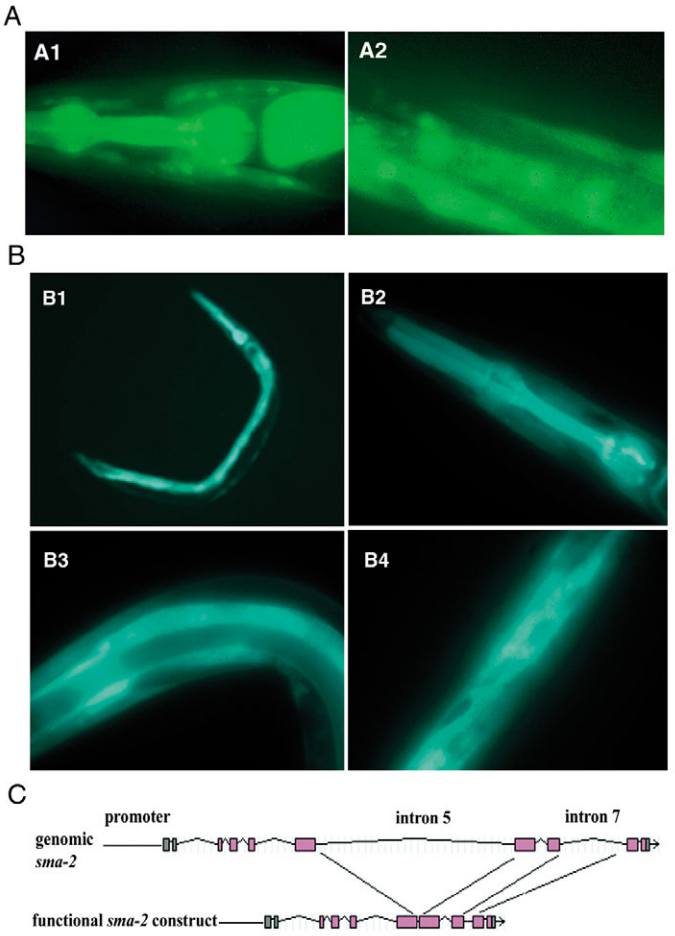

Fig. 1. Expression patterns of Smad constructs in vivo. (A) Localization of SMA-3 mutant forms. The SMA-3 AMA protein accumulates in the nucleus, similar to the accumulation of wild-type SMA-3. The other dominant-negative SMA-3 mutants have a similar localization pattern (data not shown). (B) The expression pattern of a *sma-2::gfp* transcriptional fusion gene in (B1) the whole animal, (B2) pharynx, (B3) intestine and (B4) hypodermis. (C) A functional genomic clone of *sma-2* excluding the two large introns.

regulation, they could form partially active complexes with other Smad proteins and activate negative regulators in this pathway. In this case, DME is more likely to be the strongest inhibitor because it is similar to activated Smad and has the greatest tendency to form a heteromeric complex and interact with transcription factors.

We also tested the interaction of *sma-3* mutants with *lon-1*. The *lon-1* gene encodes a PR-related protein that may be a target gene of the Sma/Mab pathway (Maduzia et al., 2002; Morita et al., 2002). It has been reported that *lon-1* expression is downregulated by the Sma/Mab signaling pathway. *lon-1(wk50)* mutants are 20% longer than wild type and their phenotype is epistatic to the small phenotype of Sma/Mab mutants (Maduzia et al., 2002) (Table 2). When the dominant-negative constructs of *sma-3* were crossed into *lon-1(wk50)*, an intermediate phenotype, smaller than wild type, is seen for all constructs (Table 2). The double-null mutant *lon-1sma-3* has a phenotype with a body length close to but longer than wild type (Maduzia et al., 2002) (Table 2). Thus, the *sma-3* C-terminal mutations are dominant negative in a *lon-1(wk50)* mutant background, causing a more severe phenotype than the *sma-3* null mutations do. This result suggests that the C-terminal mutations are different from null mutations in regulating target gene expression. Nevertheless, the worm body length is longer in the *lon-1* mutant background than in worms containing the same integrated arrays in the wild-type background. Thus, inactivation of *lon-1* partially relieves the effect of the dominant negatives. Our results are consistent with previous suggestions that *lon-1* is one, but not the only, target gene downregulated by activated SMA-3.

sma-3 C-terminal mutant forms are functional in male tail sensory ray morphogenesis

In addition to the small body size, the mutants of the Sma/Mab pathway have male tail defects. Specific sensory rays become fused and the spicules are crumpled. As most of the C-terminal mutations we generated were dominant negative in body size control, we asked whether they are also dominant negative in male tail development by crossing them into the *him-5(e1490)* background. There was no defect in any of these transgenic worms (Table 3). To test the ability of *sma-3* C-terminal mutants to rescue the male tail defects of *sma-3(wk30)* animals, we crossed the integrated arrays into *sma-3;him-5*. Although none of these mutant forms were functional in body size regulation, all of them were at least partially functional in specification of ray identity. Most surprisingly, the AMA mutation that abolishes the phosphorylation site still can rescue the male tail sensory rays. Thus, sensory ray development does not require pSMA-3. The decreased activity of the deletion suggests that a full-length SMA-3 is preferred; possibly only the backbone of the last amino acids is required.

In addition to sensory ray fusions, Sma/Mab pathway mutants have crumpled spicules at 100% penetrance. Among the C-terminal mutations, only SMA-3 DME rescues the defects in spicule morphogenesis in the *sma-3(wk30)* background. The others only improve the spicules slightly (Table 3). Thus, if we assess their ability to function in the morphogenesis of the spicules, the *sma-3* constructs meet our initial expectations. The pseudophosphorylated mutants are functional, whereas the unphosphorylatable forms are nonfunctional. In summary, body size regulation showed the least tolerance for SMA-3 C-terminal modification, sensory ray specification the greatest tolerance, and spicule morphogenesis an intermediate tolerance.

Pseudophosphorylated SMA-2 is functionally active

When the integrated *sma-3* mutant arrays were crossed into *sma-6(wk7)*, none of the constructs rescued the male tail defects (Table 3). Therefore, the upstream signal from the SMA-6 type I receptor is still required for male tail development, most likely to induce the phosphorylation of SMA-2. We wondered whether there is an absolute requirement for SMA-2 phosphorylation, or whether either SMA-2 or SMA-3 phosphorylation is sufficient for male tail development. To address this question, we assessed the ability of ppSMA-2 DID (mutated from SIS) to function in the male tail. We first needed to generate a rescuing *sma-2* clone. To test for rescue, we used the strong allele *sma-2(e297)*, as none of the sequenced *sma-2* alleles are predicted molecular nulls. A construct containing *sma-2* upstream sequences plus its

Table 3. The effects of *sma-2* and *sma-3* mutations on male tail morphogenesis

Strain	Transgene	Sensory ray fusions (%) 4&5	6&7	8&9	*n* (sides)	Crumpled spicules (%)
him-5(e1490)	None	0	0	5	120	0
	qcIs7(sma-3 DME)	0	0	5	188	0
	qcIs15(sma-3 AMA)	0	0	4	166	0
	qcIs5(sma-3 ΔSMT)	0	0	7	120	0
	qcIs4(sma-3 ΔMT)	0	0	6	110	0
sma-3(wk30); him-5(e1490)	None	12	69	28	112	100
	qcIs19(sma-3 wt)	0	0	6	100	0
	qcIs7(sma-3 DME)	0	0	7	108	5
	qcIs15(sma-3 AMA)	1	1	9	233	90
	qcIs5(sma-3 ΔSMT)	4	32	30	63	95
	qcIs4(sma-3 ΔMT)	1	1	7	74	88
sma-6(wk7); him-5(e1490)	None	12	52	29	63	100
	qcIs7(sma-3 DME)	6	63	45	200	100
	qcIs15(sma-3 AMA)	8	55	29	124	100
	qcIs5(sma-3 ΔSMT)	14	59	34	112	100
	qcIs4(sma-3 ΔMT)	6	65	30	176	100
sma-2(e297); him-5(e1490)	None	10	63	28	110	100
	qcIs39(sma-2 wt)	0	0	8	100	0
	qcIs41(sma-2 DID)	0	0	10	95	0

cDNA failed to rescue the small body size defect of *sma-2(e297)*. The genomic DNA of *sma-2* is long, including two large introns that proved difficult to clone. We created a construct without the two introns. After transforming into *sma-2(e297)*, the *sma-2* clone shows a rescuing function in both body size and male tail (Tables 2, 3). This indicates that the two introns are not required for *sma-2* function. A transcriptional fusion of *sma-2* promoter sequences with GFP shows that *sma-2* is expressed in pharynx, intestine and hypodermis, similar to the expression pattern of *sma-3* (Fig. 1B,C). This is consistent with *sma-2* and *sma-3* acting together in the signaling pathway. We generated a SMA-2 DID variant (Table 1) by PCR and transformed it into *sma-2(e297)*. Interestingly, unlike SMA-3 DME, ppSMA-2 could rescue body size (Table 2). So, SMA-2 DID is functionally active in body size control. This difference in the behaviors of SMA-2 DID and SMA-3 DME suggests that there are differential requirements for these Smad proteins in body size regulation. In the Discussion, we present a model to reconcile this apparent inconsistency.

Like ppSMA-3, ppSMA-2 can also rescue male tail sensory ray fusions and crumpled spicules (Table 3). As the pseudophosphorylation of either SMA-2 or SMA-3 could rescue male tail defects, it indicates these constructs could be independent from the receptor SMA-6. We hypothesized that the pseudophosphorylation of both SMA-2 and SMA-3 could control male tail patterning without upstream signaling. Thus, we integrated both of the constructs into *him-5* and *sma-6(wk7);him-5(e1490)*. In the wild-type background, the integrated array *qcIs43* is dominant negative in body size (data not shown), but the male tail has no defects (Table 4). Although the integrated array has the ability to rescue partially the male tail sensory ray fusions and crumpled spicules of *sma-2(e297)* or *sma-3(wk30)*, it provides no improvement in the male tail defects of *sma-6(wk7)* animals at all (Table 4). This result suggests that at least one of SMA-2 and SMA-3 must be truly phosphorylated, rather than pseudophosphorylated, for normal male tail morphogenesis. To test this hypothesis, and to exclude the possibility that male tail development also requires a Smad-independent but SMA-6-dependent signaling output, we crossed *qcIs43* into a *sma-3sma-2* double mutant. In this strain background, we were unable to homozygose the integrated array, so we scored *sma-3sma-2* double-mutant animals carrying one copy of the array. Again, the combination of ppSMA-2 and ppSMA-3 was unable to rescue the male tail defects of *sma-3sma-2* mutants (Table 4), thus confirming the difference in function between pseudophosphorylated and phosphorylated Smad.

Table 4. The effects of SMA-2 and SMA-3 pseudophosphorylation on male tail morphogenesis

Strain	Transgene	Sensory ray fusions (%) 4&5	6&7	8&9	*n* (sides)	Crumpled spicules (%)
him-5(e1490)	None	0	0	5	120	0
	qcIs43(sma-2 DID + sma-3 DME)	0	0	4	100	0
sma-2(e297); him-5(e1490)	None	10	63	28	110	100
	qcIs43(sma-2 DID + sma-3 DME)	9	9	49	110	100
sma-3(wk30); him-5(e1490)	None	12	69	28	112	100
	qcIs43(sma-2 DID + sma-3 DME)	2	4	34	100	25
sma-6(wk7); him-5(e1490)	None	12	52	29	63	100
	qcIs43(sma-2 DID + sma-3 DME)	11	51	22	120	100
sma-3(e491) sma-2(e502); him-5(e1490)	None	32	72	52	50	100
	qcIs43(sma-2 DID + sma-3 DME) / +	24	69	61	76	100

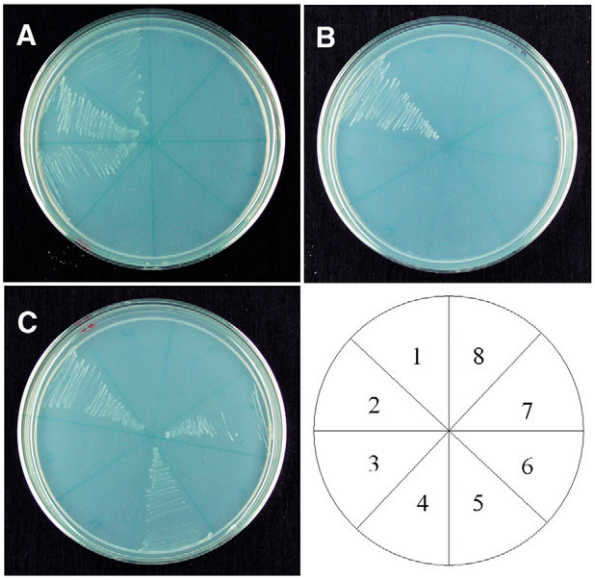

Fig. 2. The yeast two-hybrid test of the interaction between LIN-31 and SMA-3 or SMA-2. (A) An interaction can be detected between SMA-3 and LIN-31 by using a His selection plate (50 mM 3AT): (1) *sma-3-AMA:lin-31*, (2) *sma-3-DME:lin-31*, (3) *sma-3:lin-31*, (4) *lin-31*:vector, (5) *sma-3-AMA*:vector, (6) *sma-3-DME*:vector, (7) *sma-3:vector* and (8) vector:vector. (B) There was no detectable interaction between SMA-2 and LIN-31 when using the His selection plate (25 mM 3AT). (1) *sma-3*:vector, (2) *sma-3:lin-31*, (3) *lin-31*:vector, (4) vector:vector, (5) *sma-2:lin-31*, (6) *sma-2*:vector, (7) *sma-2-DID*:*lin-31* and (8) *sma-2-DID*:vector. (C) Both MH1 and MH2 domains of SMA-3 can interact with LIN-31, as detected using the His selection plate (25 mM 3AT): (1) *sma-3*:vector, (2) *sma-3*:*lin-31*, (3) *lin-31*:vector, (4) vector:vector, (5) *sma-3* MH2:*lin-31*, (6) *sma-3* MH2: vector, (7) *sma-3* MH1:*lin-31* and (8) *sma-3* MH1:vector. Note, the *sma-2* or *sma-3* cDNA was inserted into pPDleu vector and *lin-31* cDNA was inserted into pPC86 vector. The yeast strain used for all of the tests was Mav203.

SMA-3 interacts with LIN-31

lin-31 is implicated in the Sma/Mab pathway because *lin-31* mutant males have crumpled spicules identical to *sma-3* mutants (Baird and Ellazar, 1999). *lin-31* encodes a forkhead transcription factor (Miller et al., 1993). We tested for molecular interactions between LIN-31 and the Smads using the yeast two-hybrid system. We detected that wild-type SMA-3 interacts with the forkhead transcription factor LIN-31. SMA-3 DME interacts with LIN-31 more strongly, while SMA-3 AMA interacts more weakly (Fig. 2A). This result implies that the phosphorylation of the SMA-3 C terminus could also enhance its interaction with LIN-31. No interaction between LIN-31 and wild-type SMA-2 or ppSMA-2 is detectable (Fig. 2B). The interaction of SMA-4 and LIN-31 could not be tested because of the self-activation of SMA-4. When we tested whether SMA-3 MH1 and MH2 domains are required for the interaction, we found that both MH1 and MH2 (wild type) interact with LIN-31, but that the interaction between MH1 and LIN-31 is weaker (Fig. 2C). The fact that *lin-31* mutants have crumpled spicules, but are not small, and the male tail sensory rays are normal (Baird and Ellazar, 1999) suggests that the interaction between SMA-3 and LIN-31 is only required for the development of the spicules. It has been reported that the forkhead transcription factor Fast-1 has a Smad interacting motif (SIM) (Germain et al., 2000). In addition, a novel Smad2 interaction motif, the Fast/FoxH1 motif (FM) is present in all known Fast/FoxH1 family members (Randall et al., 2004). The FM is necessary and sufficient to bind active Smad2:Smad4 complexes and discriminates between activated and unactivated Smad2. The FM is not conserved in *C. elegans* LIN-31, but there could be other motifs in LIN-31 that interact strongly with activated SMA-3 or ppSMA-3.

The SMA-3 mutations differ in their abilities to turn on a feedback loop

When GFP is inserted at the C terminus of SMA-3, the construct does not have much activity, but accumulates at a high level. Functional SMA-3 can downregulate this SMA-3::GFPC accumulation by a negative-feedback loop (Wang et al., 2002). We tested whether the SMA-3 C-terminal mutants could turn on the feedback loop. We co-injected the *sma-3::gfp* C-terminal fusion with the mutated *sma-3* genes. The fluorescence intensity shows that the SMA-3 AMA and SMA-3 ΔSMT downregulate SMA-3::GFPC protein accumulation just like wild-type SMA-3 does (Fig. 3A-D). But, with SMA-3 DME, the fluorescence of SMA-3::GFPC is almost undetectable (Fig. 3E). Thus, SMA-3 DME is a strong inhibitor of the protein accumulation. In summary, the C-terminal mutations retain the ability to turn on the feedback loop that induces SMA-3 degradation. This activity may be one of the causes of their dominant-negative phenotypes in the presence of wild-type SMA-3.

The C terminus of SMA-4 is not important for its activity

The C-terminal amino acid residues of SMA-4 are two serines (SS), whereas those of its homolog Smad4 are leucine and aspartic acid (LD). To test whether these C-terminal serines have any significant function, we produced several mutations of SMA-4. The SS was changed into SSIS (more like an R-Smad), DD (negatively charged) and AA (remove the hydroxyl groups) (Table 1). These constructs were introduced into *sma-4(e729)* mutants, which carry a null allele with a premature termination codon in *sma-4* (Wang et al., 2002). All of the three constructs function as well as wild-type SMA-4 in body size regulation (Table 2). The construct with SSIS could not substitute for any other Smads, as it failed to rescue the small body size of *sma-2* or *sma-3* mutants (data not shown). This suggests, not surprisingly, that the identity of Smads is not determined by the most C-terminal amino acids, but by the internal sequences that are necessary for receptor activation and subtype-specific functions. The results also tell us that the C terminus of SMA-4 is different from that of SMA-2 or SMA-3, in that it is dispensable for SMA-4 function. In the crystal structure of the Smad4 MH2 domain, the C terminus is randomly located (Shi et al., 1997), unlike that of pSmad2 (Wu et al., 2001b). It is likely that the C terminus of Co-Smad is not involved in complex formation or other intermolecular interactions.

Discussion

The role of the C terminus of SMA-3

Several functional roles have been ascribed to the phosphorylation of R-Smad C termini by type I receptors,

most notably the stimulation of heteromeric complex formation and nuclear accumulation. Heteromeric complex formation is driven by the interaction of the phosphorylated C terminus with a positively charged surface of a neighboring subunit (Chacko et al., 2004). Nuclear accumulation occurs in the context of dynamic nucleocytoplasmic shuttling, which occurs in both stimulated and unstimulated cells (Reguly and Wrana, 2003; Xu et al., 2003; Nicolas et al., 2004). Phosphorylation is thus not required for nuclear import but rather for nuclear accumulation of Smad complexes, possibly by altering the relative affinity of Smad binding to cytoplasmic and nuclear partners (Xu et al., 2000). To test the functional roles of Smad C termini in vivo, we have created SMA-2 and SMA-3 mutant forms and introduced them into wild-type and mutant *C. elegans* strains. Our results are consistent with a role for C-terminal modification in Smad complex formation, but not in R-Smad nuclear accumulation. The constitutive nuclear accumulation of Smads in *C. elegans* could reflect a relative lack of cytoplasmic retention mechanisms. Furthermore, we suggest that the phosphorylation of the C terminus may play a role in transcription co-factor binding. Precedence for such a role comes from the specific interaction of activated Smad2 with Fast1 via the FM Smad-interaction motif (Randall et al., 2004). If the C-terminal mutants have different affinities for tissue-specific transcription co-factors, then this would explain their differential abilities to rescue developmental outcomes (Table 5). Our yeast two-hybrid experiments testing the interactions of LIN-31 with SMA-3 mutant forms support this conclusion.

ppSMA-3 was functional in some of the assays we performed but not in others. Its ability to turn on a negative-feedback loop in the hypodermis suggests that it is partially functional in this tissue; it failed, however, to rescue *sma-3* mutant small body size. Thus, a physiologically phosphorylated C terminus is probably necessary for transcriptional regulation of some target gene(s) functioning in body size regulation. The relevant transcription co-factors may have a high affinity only for phosphorylated SMA-3. As hypodermal expression of *sma-3* is necessary and sufficient to rescue the body size of *sma-3(wk30)* (Wang et al., 2002), the transcription factors responsible for body size should be expressed in hypodermal cells. One candidate transcription factor is the zinc-finger protein SMA-9 (Liang et al., 2003), but we were unable to detect any interaction between SMA-9 and the Smad proteins using the yeast two-hybrid system (data not shown). In spicule formation, the forkhead transcription factor LIN-31 may function with the Smads (Baird and Ellazar, 1999). SMA-3 DME is functional in spicule morphogenesis and capable of interacting with LIN-31 in the yeast two-hybrid assay. This interaction could be strong enough to allow proper spicule morphogenesis in vivo. In the sensory rays, the full-length, but non-phosphorylatable SMA-3 is sufficient to rescue the ray fusions. This result suggests that phosphorylation of SMA-3 is not required for interaction with the relevant transcription co-factors involved in sensory ray development. Thus, we believe that it is likely that the binding requirements of specific transcription factors determine the level of SMA-3 construct activities in different cell types.

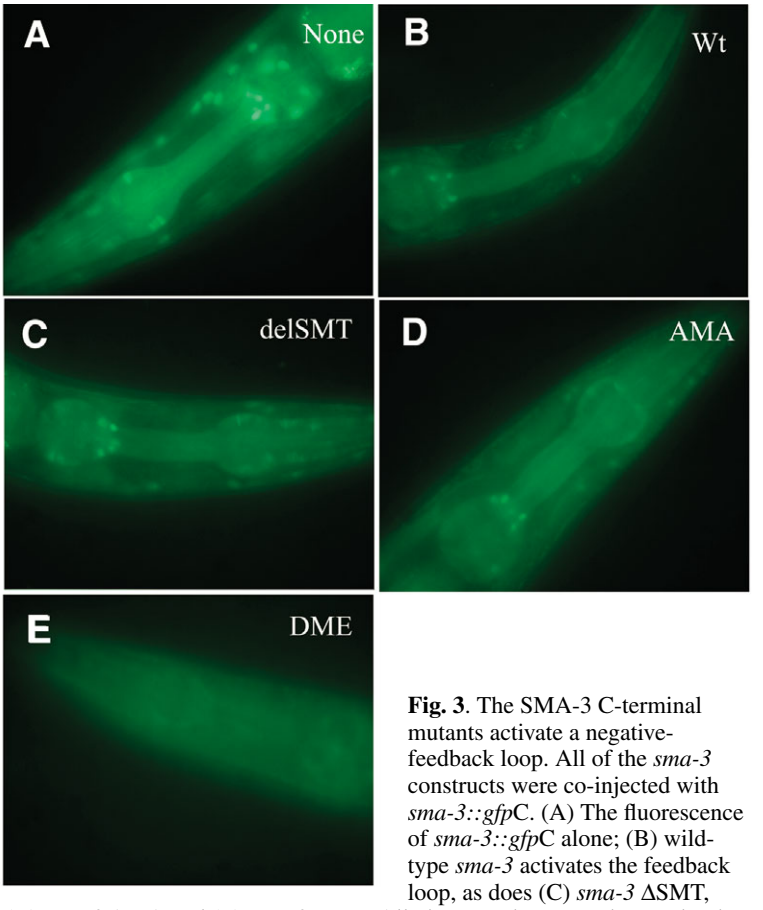

Fig. 3. The SMA-3 C-terminal mutants activate a negative-feedback loop. All of the *sma-3* constructs were co-injected with *sma-3::gfp*C. (A) The fluorescence of *sma-3::gfp*C alone; (B) wild-type *sma-3* activates the feedback loop, as does (C) *sma-3* ΔSMT, (D) *sma-3* AMA and (E) *sma-3* DME. All photographs were taken under the same conditions with the same exposure time.

Table 5. The combinations of SMA-2 and SMA-3 with different phosphorylation states have different effects on body size, male tail sensory rays, spicules and feedback loop

Phosphorylation status	Body size	Sensory rays	Spicules	Feedback loop
SMA-2-OH, SMA-3-OH	–	–	–	–
SMA-2-P, SMA-3-P	+	+	+	+
SMA-2-P, SMA-3-DME	–	+	+	+
SMA-2-P, SMA-3-AMA	–	+	–	+
SMA-2-OH, SMA-3-DME	–	–	–	ND
SMA-2-DID, SMA-3-P	+	+	+	ND
SMA-2-DID, SMA-3-DME	–	–	–	ND

P, phosphorylated C-terminal residues; –OH, wild-type unphosphorylated C terminus; +, functional; –, non-functional; ND, not determined.

Complex formation by the SMA proteins

Smad complex formation has been studied by using gel shift, column elution and crystallization methods, and different models have been suggested. The R-Smad:Co-Smad heteromeric complex has been proposed to be either a dimer (Jayaraman and Massague, 2000; Wu et al., 2001a; Inman and

Hill, 2002) or a trimer (Kawabata et al., 1998; Chacko et al., 2001; Qin et al., 2001; Wu et al., 2001b; Inman and Hill, 2002; Chacko et al., 2004). When *sma-2, sma-3* and *sma-4* were first identified in *C. elegans*, the heterotrimer model was suggested because pathway activity requires all three of them (Savage et al., 1996). Double and triple mutants of *sma-2*, *sma-3* and *sma-4* do not have more severe phenotypes than the single mutants, indicating that in animals expressing only one or two of the three Smads no pathway function is detectable (Savage-Dunn et al., 2000). Although we cannot formally exclude the possibility that SMA-2 and SMA-3 form complexes with SMA-4 independently, such complexes have no observable function. A great deal of biochemical evidence also supports the heterotrimer model. In the crystal structure of the Smad4 MH2 domain (Shi et al., 1997), the protein forms a homotrimer. In the crystal structure of Smad1 or pSmad2, the C-terminal tail interacts with a positively charged surface of a neighboring subunit in a homotrimer manner (Qin et al., 2001; Wu et al., 2001b). Similarly, the pSmad2:Smad4 and pSmad3:Smad4 crystal structures show a heterotrimer in which the phosphorylated R-Smad C termini interact with a neighboring subunit (Chacko et al., 2004). Based on this model, the Smad complex in *C. elegans* could be formed through similar interactions. In the sequence alignment, we find all of the positively charged residues are highly conserved among *C. elegans* Smads.

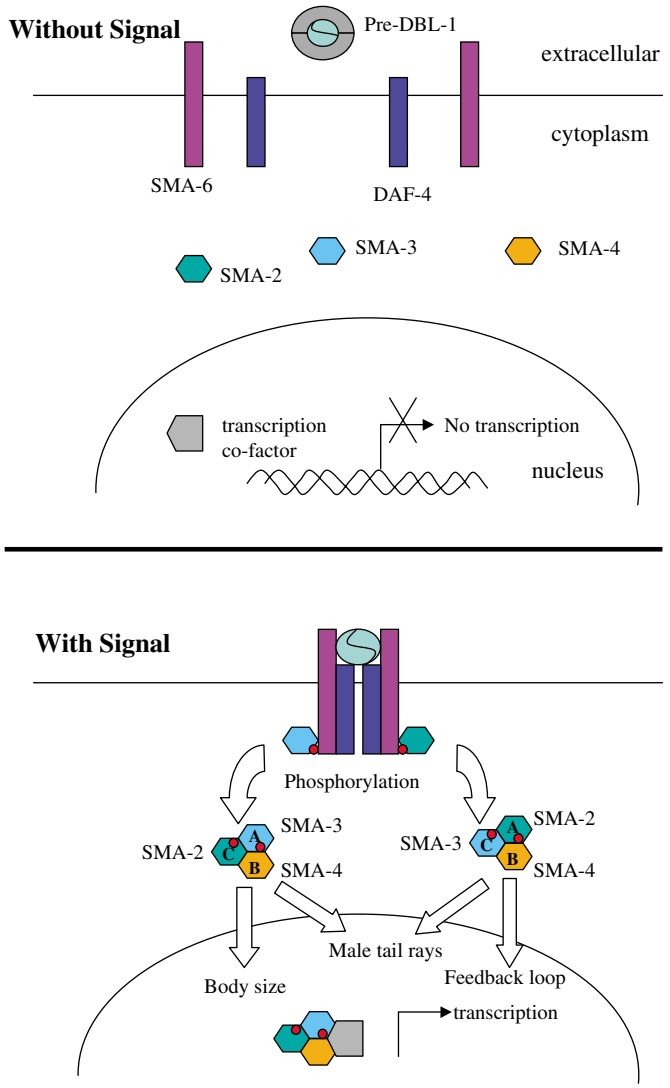

Fig. 4. Proposed model of the functional complexes of *C. elegans* Smads. The body size control requires a SMA-3:SMA-4:SMA-2 complex and the feedback loop needs a SMA-2:SMA-4:SMA-3 complex; subunits are shown in an A,B,C configuration, as defined by Chacko et al. (Chacko et al., 2004).

In the heterotrimer, the evidence suggests that two R-Smads will interact with one Co-Smad. The Smad2-Smad4 trimer contains one Smad4 and two Smad2 molecules (Inman and Hill, 2002). The complex of Smad4 and ppSmad3 shows a similar ratio (Chacko et al., 2001). The pSmad2:Smad4 and pSmad3:Smad4 crystal structures contain a 2:1 R-Smad:Co-Smad ratio (Chacko et al., 2004). Finally, a trimer formed by Smad2, Smad3 and Smad4 (Feng et al., 2000) has also been reported. The simplest model of heterotrimer formation would suggest that both R-Smad subunits are phosphorylated. We have found, however, that in *C. elegans* male tail sensory rays, phosphorylatable SMA-3 is not required for function (Tables 3, 5). Thus, it is possible that a Smad heterotrimer may contain one pR-Smad and one unphosphorylated R-Smad. In the case of male sensory rays, the functional complex must contain both SMA-2 and SMA-3, but only one of them needs to be phosphorylated. This finding has implications for the interpretation of morphogen gradients in other contexts. At high levels of ligand, cells may contain a large proportion of Smad heterotrimers containing two pR-Smads, whereas at lower levels of ligand more of the trimers may contain a single pR-Smad and a single unphosphorylated R-Smad. Thus, the Smad heterotrimer composition may provide a direct measure of ligand concentration that can then be translated into differential gene expression.

Our results with SMA-2 DID and SMA-3 DME indicate that SMA-2 DID can rescue the body size defect of a *sma-2* mutant, whereas SMA-3 DME cannot rescue the body size defect of a *sma-3* mutant (Table 5). This difference suggests that the complex containing SMA-2 DID and pSMA-3 is functionally different from the one containing pSMA-2 and SMA-3 DME. One model that can reconcile all of our data is presented in Fig. 4. In a normal heterotrimer, there are two possible configurations of the subunits. In one, the phosphorylated C terminus of SMA-2 interacts with SMA-4, that of SMA-3 interacts with SMA-2, and the unphosphorylated C terminus of SMA-4 interacts with SMA-3. In the other configuration, the phosphorylated C terminus of SMA-3 interacts with SMA-4, that of SMA-2 with SMA-3, and the SMA-4 C terminus interacts with SMA-2. Chacko et al. (Chacko et al., 2004) have designated the two R-Smad subunits in a heterotrimer as subunits A and C, and the Co-Smad as subunit B. The AB interface is that of the pR-Smad C terminus with Co-Smad, and it forms more favorable interactions than that of the CA interface between R-Smads. It is possible that the interaction between a pR-Smad (A subunit) and SMA-4 (B subunit) drives complex formation, leading to the recruitment of a second R-Smad (C subunit). According to this model, the C subunit R-Smad need not be phosphorylated. Thus, in the SMA-2 DID background, there would be an excess of pSMA-3:SMA-4:ppSMA-2 complexes relative to ppSMA-2:SMA-4:pSMA-3 complexes. Conversely, in the SMA-3 DME background, there would be an excess of pSMA-2:SMA-4:ppSMA-3 complexes. For some target gene(s) involved in body size regulation, we hypothesize that the configuration of

SMA-3:SMA-4:SMA-2 is required for normal function. By contrast, the SMA-2:SMA-4:SMA-3 configuration may be sufficient for the feedback loop, which can be triggered by SMA-3 DME. In male tail development, both kinds of trimers are functional. Thus, different branches of the pathway may depend on different complexes.

We thank Stuart Kim for providing the *lin-31* clones, Richard Kolesnick for the use of a cesium source, Joni Seeling and PoKay Ma for critical reading of the manuscript. This research was supported by RPG 98-230-01-DDC and RSG 98-230-04-DDC from the American Cancer Society and a PSC-CUNY research award to C. S.-D and by HD43156 from the NIH and a New Scholar in Aging award from the Ellison Medical Foundation to W.A.M. Some *C. elegans* mutant strains were obtained from the *Caenorhabditis* Genetics Center, which is supported by the NIH National Center for Research Resources (NCRR). This work was carried out in partial fulfillment of the requirements for a PhD degree from the Graduate Center of the City University of New York (J.W.).

References

Abdollah, S., Macías-Silva, M., Tsukazaki, T., Hayashi, H., Attisano, L. and Wrana, J. L. (1997). TβRI phosphorylation of Smad2 on Ser^{465} and Ser^{467} is required for Smad2-Smad4 complex formation and signaling. *J. Biol. Chem.* **272**, 27678-27685.

Attisano, L. and Wrana, J. L. (2002). Signal transduction by the TGF-β superfamily. *Science* **296**, 1646-1647.

Baird, S. E. and Ellazar, S. A. (1999). TGFβ-like signaling and spicule development in *Caenorhabditis elegans*. *Dev. Biol.* **212**, 93-100.

Brenner, S. (1974). The genetics of *Caenorhabditis elegans*. *Genetics* **77**, 71-94.

Chacko, B. M., Qin, B., Correia, J. J., Lam, S. S., de Caestecker, M. P. and Lin, K. (2001). The L3 loop and C-terminal phosphorylation jointly define Smad protein trimerization. *Nat. Struct. Biol.* **8**, 248-253.

Chacko, B. M., Qin, B. Y., Tiwari, A., Shi, G., Lam, S., Hayward, L. J., de Caestecker, M. and Lin, K. (2004). Structural basis of heteromeric Smad protein assembly in TGF-β signaling. *Mol. Cell* **15**, 813-823.

Estevez, M., Attisano, L., Wrana, J. L., Albert, P. S., Massagué, J. and Riddle, D. L. (1993). The *daf-4* gene encodes a bone morphogenetic protein receptor controlling C. elegans dauer larva development. *Nature* **365**, 644-649.

Feng, X. H., Lin, X. and Derynck, R. (2000). Smad2, Smad3 and Smad4 cooperate with Sp1 to induce p15(Ink4B) transcription in response to TGF-β. *EMBO J.* **19**, 5178-5193.

Germain, S., Howell, M., Esslemont, G. M. and Hill, C. S. (2000). Homeodomain and winged-helix transcription factors recruit activated Smads to distinct promoter elements via a common Smad interaction motif. *Genes Dev.* **14**, 435-451.

Hata, A., Lo, R. S., Wotton, D., Lagna, G. and Massagué, J. (1997). Mutations increasing autoinhibition inactivate tumour suppressors Smad2 and Smad4. *Nature* **388**, 82-87.

Inman, G. J. and Hill, C. S. (2002). Stoichiometry of active Smad-transcription factor complexes on DNA. *J. Biol. Chem.* **277**, 51008-51016.

Jayaraman, L. and Massague, J. (1998). Distinct oligomeric states of SMAD proteins in the transforming growth factor-β pathway. *J. Biol. Chem.* **275**, 40710-40717.

Kawabata, M., Inoue, H., Hanyu, A., Imamura, T. and Miyazono, K. (1998). Smad proteins exist as monomers in vivo and undergo homo- and hetero-oligomerization upon activation by serine/threonine kinase receptors. *EMBO J.* **17**, 4056-4065.

Liang, J., Lints, R., Foehr, M. L., Tokarz, R., Yu, L., Emmons, S. W., Liu, J. and Savage-Dunn, C. (2003). The *Caenorhabditis elegans schnurri* homolog, *sma-9,* mediates stage- and cell type-specific responses to *dbl-1* BMP-related Signaling. *Development* **130**, 6453-6464.

Liu, X., Sun, Y., Constantinescu, S. N., Karam, E., Weinberg, R. A. and Lodish, H. F. (1997). Transforming growth factor β-induced phosphorylation of Smad3 is required for growth inhibition and transcriptional induction in epithelial cells. *Proc. Natl. Acad. Sci. USA* **94**, 10669-10674.

Maduzia, L. L., Gumienny, T. L., Zimmerman, C. M., Wang, H., Shetgiri, P., Krishna, S., Roberts, A. F. and Padgett, R. W. (2002). *lon-1* regulates *Caenorhabditis elegans* body size downstream of the *dbl-1* TGF-β signaling pathway. *Dev. Biol.* **246**, 418-428.

Massagué, J. (2003). Integration of Smad and MAPK pathways: a link and a linker revisited. *Genes Dev.* **17**, 2993-2997.

Massagué, J. and Wotton, D. (2000). Transcriptional control by the TGF-β/Smad signaling system. *EMBO J.* **19**, 1745-1754.

Mello, C. C., Kramer, J. M., Stinchcomb, D. T. and Ambros, V. (1991). Efficient gene transfer in *C. elegans*: extrachromosomal maintenance and integration of transforming sequences. *EMBO J.* **10**, 3959-3970.

Miller, L. M., Gallegos, M. E., Morisseau, B. A. and Kim, S. K. (1993). *lin-31*, a *Caenorhabditis elegans* HNF-3/fork head transcription factor homolog, specifies three alternative cell fates in vulval development. *Genes Dev.* **7**, 933-947.

Morita, K., Flemming, A. J., Sugihara, Y., Mochii, M., Suzuki, Y., Yoshida, S., Wood, W. B., Kohara, Y., Leroi, A. M. and Ueno, N. (2002). A *Caenorhabditis elegans* TGF-β, DBL-1, controls the expression of LON-1, a PR-related protein, that regulates polyploidization and body length. *EMBO J.* **21**, 1063-1073.

Moustakas, A., Souchelnytskyi, S. and Heldin, C. H. (2001). Smad regulation in TGF-β signal transduction. *J. Cell Sci.* **114**, 4359-4369.

Nicolas, F. J., De Bosscher, K., Schmierer, B. and Hill, C. S. (2004). Analysis of Smad nucleocytoplasmic shuttling in living cells. *J. Cell Sci.* **117**, 4113-4125.

Patterson, G. I. and Padgett, R. W. (2000). TGF β-related pathways: roles in *Caenorhabditis elegans* development. *Trends Genet.* **16**, 27-33.

Petritsch, C., Beug, H., Balmain, A. and Oft, M. (2000). TGF-β inhibits p70 S6 kinase via protein phosphatase 2A to induce G(1) arrest. *Genes Dev.* **14**, 3093-3101.

Qin, B. Y., Chacko, B. M., Lam, S. S., de Caestecker, M. P., Correia, J. J. and Lin, K. (2001). Structural basis of Smad1 activation by receptor kinase phosphorylation. *Mol. Cell* **8**, 1303-1312.

Randall, R. A., Howell, M., Page, C. S., Daly, A., Bates, P. A. and Hill, C. S. (2004). Recognition of phosphorylated-Smad2-containing complexes by a novel Smad interaction motif. *Mol. Cell Biol.* **24**, 1106-1121.

Reguly, T. and Wrana, J. L. (2003). In or out? The dynamics of Smad nucleocytoplasmic shuttling. *Trends Cell Biol.* **13**, 216-220.

Savage, C., Das, P., Finelli, A. L., Townsend, S. R., Sun, C. Y., Baird, S. E. and Padgett, R. W. (1996). *Caenorhabditis elegans* genes *sma-2*, *sma-3*, and *sma-4* define a conserved family of transforming growth factor β pathway components. *Proc. Natl. Acad. Sci. USA* **93**, 790-794.

Savage-Dunn, C. (2001). Targets of TGF β-related signaling in *Caenorhabditis elegans*. *Cytokine Growth Factor Rev.* **12**, 305-312.

Savage-Dunn, C., Tokarz, R., Wang, H., Cohen, S., Giannikas, C. and Padgett, R. W. (2000). SMA-3 smad has specific and critical functions in DBL-1/SMA-6 TGFβ-related signaling. *Dev. Biol.* **223**, 70-76.

Shi, Y. and Massagué, J. (2003). Mechanisms of TGF-β signaling from cell membrane to the nucleus. *Cell* **113**, 685-700.

Shi, Y., Hata, A., Lo, R. S., Massagué, J. and Pavletich, N. P. (1997). A structural basis for mutational inactivation of the tumour suppressor Smad4. *Nature* **388**, 87-93.

Souchelnytskyi, S., Tamaki, K., Engström, U., Wernstedt, C., ten Dijke, P. and Heldin, C. H. (1997). Phosphorylation of Ser^{465} and Ser^{467} in the C terminus of Smad2 mediates interaction with Smad4 and is required for transforming growth factor-β signaling. *J. Biol. Chem.* **272**, 28107-28115.

Wakefield, L. M. and Roberts, A. B. (2002). TGF-beta signaling: positive and negative effects on tumorigenesis. *Curr. Opin. Genet. Dev.* **12**, 22-29.

Wang, J., Tokarz, R. and Savage-Dunn, C. (2002). The expression of TGFβ signal transducers in the hypodermis regulates body size in *C. elegans* *Development* **129**, 4989-4998.

Wu, J. W., Fairman, R., Penry, J. and Shi, Y. (2001a). Formation of a stable heterodimer between Smad2 and Smad4. *J Biol. Chem* **276**, 20688-20694.

Wu, J. W., Hu, M., Chai, J., Seoane, J., Huse, M., Li, C., Rigotti, D. J., Kyin, S., Muir, T. W., Fairman, R. et al. (2001b). Crystal structure of a phosphorylated Smad2. Recognition of phosphoserine by the MH2 domain and insights on Smad function in TGF-β signaling. *Mol. Cell* **8**, 1277-1289.

Xu, L., Chen, Y.-G. and Massague, J. (2000). The nuclear import function of Smad2 is masked by SARA and unmasked by TGFβ-dependent phosphorylation. *Nat. Cell Biol.* **2**, 559-562.

Xu, L., Alarcon, C., Col, S. and Massague, J. (2003). Distinct domain utilization of Smad3 and Smad4 for nucleoporin interaction and nuclear import. *J. Biol. Chem.* **278**, 42569-42577.